Experimental and Simulation Results for Sliding Mode Dynamic Wind Turbine Control using a DC Chopper

G. Riahy[1], P. Freere[2,3], D.G Holmes[4]

1. No. 301, 12 Moharran Ave, Shahre-Kord 88167, Iran
2. Biomass Energy Services and Technology, 56 Gindurra Rd, Somersby NSW 2570, Australia
3. RRC, Chonnam National University, Kwangju, Korea
4. P.E.G., Monash University, Clayton, Victoria 3168, Australia

All this work has been performed at P.E.G. (Power Electronics Group) in Monash University, Australia.

ABSTRACT: *Wind speeds can vary rapidly and wind turbines cannot easily follow these variations because of their inertia and aerodynamic characteristics. For maximum energy extraction, the turbine blades should operate at their optimum tip speed ratio, but with rapid changes in wind speed, this is usually not possible. To improve the energy extraction from turbulent wind, it is necessary to establish an effective measure of the high frequency component of the wind, and then to use this measure to optimise the operation of the turbine controller for maximum energy extraction. This paper presents an approach for combining readings from three anemometers into a composite wind speed measurement, and using this signal to control the operation of a permanent magnet generator to achieve maximum energy extraction. The method combines simulation and experimental investigations into a heuristic algorithm, and demonstrates its effectiveness with field trials.*

1.0 INTRODUCTION

A prime interest in wind turbine control is to be able to increase the energy captured from the wind. But because of their inertia, most wind turbines cannot access the high frequency component of the wind, since they cannot maintain their optimum turbine tip speed ratio from moment to moment [Leithhead '89] [Torbjorn '93]. However, these high frequency components are often of high wind velocity and hence have the potential to substantially contribute to the energy that can be captured by the wind turbine.

To access this high frequency wind energy, two problems must be overcome. Firstly, a suitable measurement is required to identify to a turbine controller that part of the high frequency wind energy that can be usefully extracted.

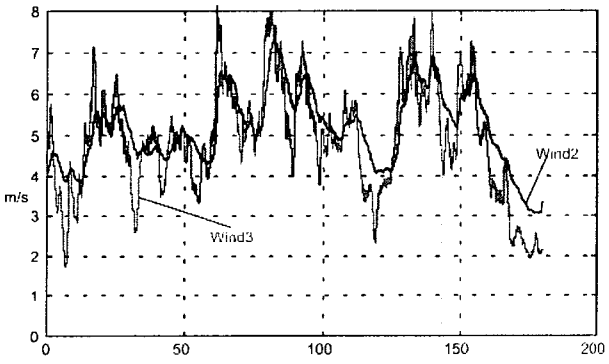

Figure 1.1 The wind speeds measured by the two nearby anemometers, $Wind_2$ and $Wind_3$.

Secondly, a control strategy is then required to maximise the extraction of this high frequency energy.

The usual parameter for determining wind energy is wind speed, typically measured using a rotating cup anemometer. But rotating cup anemometers have widely differing frequency characteristics, as shown in Fig. 1.1 and can even have a worse frequency response than the wind turbine itself. Hence a simple wind speed measurement is inadequate to determine the high frequency wind energy component. Furthermore, it is difficult even to measure the frequency response of the anemometer itself.

In this paper a solution to this problem is presented that combines readings from 3 anemometers of differing frequency response into one measured quantity. This quantity is then heuristically filtered to create a composite wind speed indicator that is used as a reference input into the turbine controller to increase the energy extracted.

The filter algorithm was derived by comparing an accurate simulation model of the Rutland wind turbine shown in Fig. 1.2, against experimental results. The simulation model was driven by a wind "speed" parameter made up of the anemometer field readings combined together and fed through the heuristic filter. The filter algorithm was then adjusted until the rotor speed of the simulation matched the rotor speed of the experimental system that was recorded at the same time as the wind speed readings were taken.

Having established the high frequency wind speed reference signal, it is then possible to investigate how the operation of a turbine controller might be optimised to maximise the

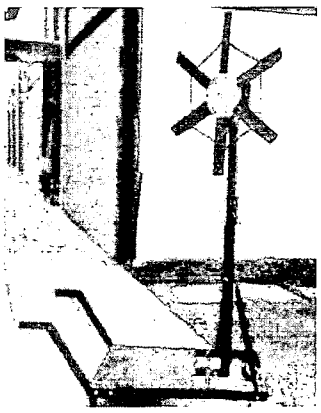

Figure 1.2 Rutland 910 wind turbine used for the experimental work.

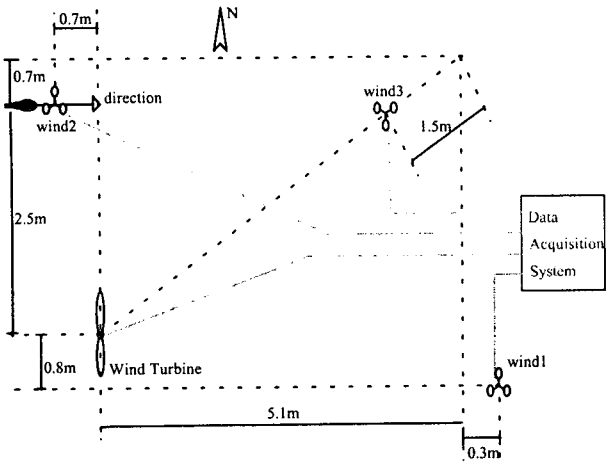

Figure 2.1 The wind turbine and anemometer physical locations.

energy extracted from turbulent wind that has a significant high frequency component.

2.0 EXPERIMENTAL SYSTEM

The turbine used was a Rutland 910 turbine (Fig. 1.1) with a small diameter of 95cm. It is rated at 50W in a $10ms^{-1}$ wind speed and designed to charge a 12V battery. It should be noted that the advantage of using a small turbine is that it will not experience much wind shear, and hence the wind velocity can be considered to be constant across the cross sectional area of the turbine.

The experimental system was set up on the roof of the Monash University Electrical Engineering building for convenient visual monitoring of the system. Due to the prevalence of nearby buildings, the wind was known to be turbulent. The anemometers were placed as shown in Fig. 2.1, with the downwind units placed just over 5 turbine diameters away to avoid turbulence created by the turbine, as recommended by [Freris '90].

The turbine load was kept constant as a 12V battery load,

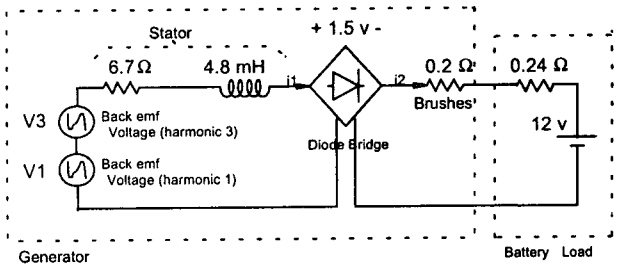

Figure 3.1 Generator electrical model.

implemented as a power supply and a series resistance.

Fig 2.2 shows a block diagram of the entire experimental system, showing the interconnection between the various system components. The effective wind speed is determined from the three anemometers by the data acquisition computer, which also controls the power output from the turbine via a dc-dc converter.

3.0 MODEL OF TURBINE SYSTEM

A true dynamic model of a turbine's aerodynamic performance is difficult. However, a number of authors have successfully used the steady state model of a turbine's power coefficient expressed as a function of the tip speed ratio, as a dynamic model [Rosen '91, Wilmshurst '88]. This is the approach taken in this paper.

Initially, the turbine generator performance was tested on the bench and and accurate electrical and mechanical model of the permanent magnet generator as per Fig. 3.1 was developed from these results. Then the turbine was placed in a wind tunnel and its aerodynamic performance was modelled by subtracting the predicted contribution of the generator (both electrically and mechanically) from the measured electrical output.

For this generator, with a nominal output current at rated power (50W) of approximately 4A, the resistive losses are 110W. This produces a relatively low efficiency of 30%.

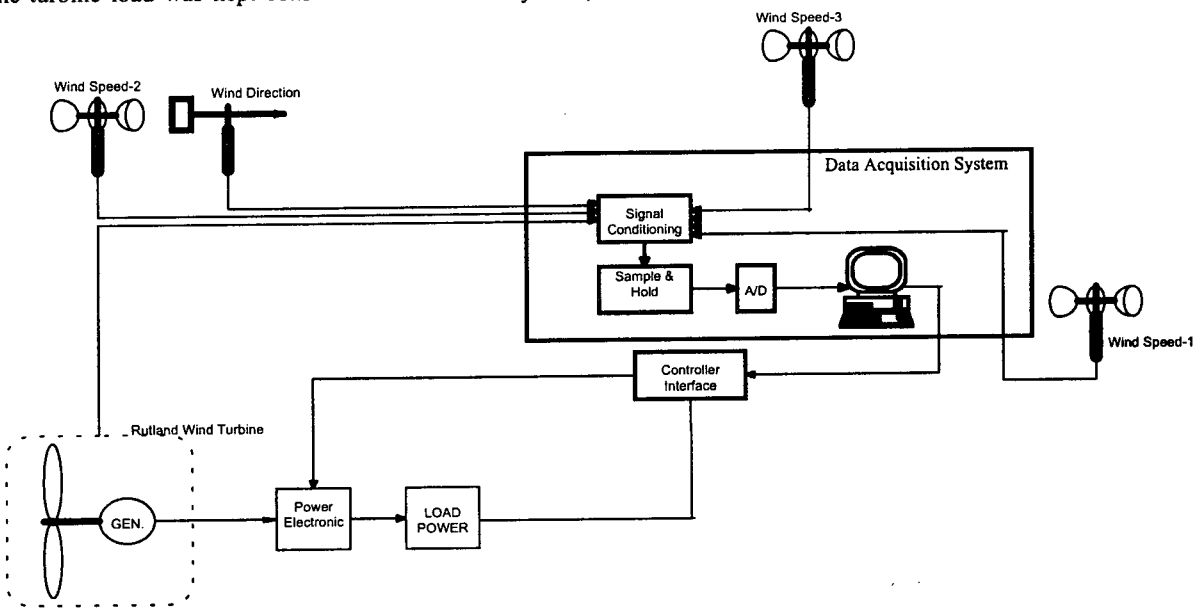

Figure 2.2 The block diagram of the system. The data acquisition system is high lighted in the figure. The power electronic converter is a dc chopper.

The power coefficient of a turbine is defined as the ratio of the power delivered by the blades to the available power in the wind [McIver 95]. It can be modelled as a polynomial [Borowy 97] and a cubic polynomial has been found to be adequate in this case.

The available power in the wind and from the turbine blades is defined in equations 3.1 and 3.2 .

$$P = \tfrac{1}{2} \rho A v^3 \quad (3.1)$$

$$P_t = \tfrac{1}{2} c_p \rho A v^3 \quad (3.2)$$

P = power available in the wind (W)
P_t = power from the turbine blades
ρ = density of air (kg/m^3)
A = cross sectional area of the turbine (m^2)
v = wind velocity (m/s)
c_p = turbine power coefficient

Fig. 3.2 shows the measured power of the turbine as a function of the tip speed ratio, together with the best fit cubic polynomial that is used to model the curve (shown above the curve). The optimum tip speed ratio (lamda) can be seen to be 2.4 and the maximum power coefficient c_p is 0.22.

The mechanical model of the generator includes its friction, windage and inertia. The friction, windage and inertia of the generator was measured and the inertia of each of the 6 blades was then calculated from their weight. Details are given in the appendix.

4.0 WIND SPEED MEASUREMENT ALGORITHM

As is normal practice, the first step in establishing the wind speed measurement system was to confirm that the anemometer readings in their positions away from the turbine correlated well with the wind speed measured at the turbine position.

Once this was confirmed, the readings were integrated and heuristically filtered to create a combined low and high frequency wind speed measurement. As discussed earlier, the validity of the filtering was confirmed by correlating [Press '92] the simulated turbine speed against the experimental turbine speed under the same wind conditions. The match was considered acceptable only when the correlation coefficient was greater than 90% [Harrap '93]. Note that this validation could only be done when the wind direction was measured to be constant, because the algorithm has no mechanism to compensate for possible rotor yaw as the wind direction changes.

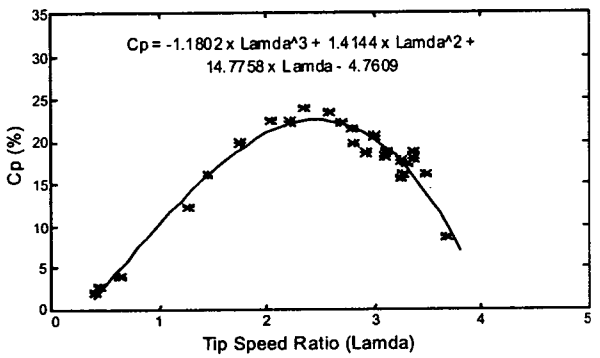

Figure 3.2 The power coefficient curve for the Rutland wind turbine as a function of the tip speed ratio. Optimum tip speed ratio = 2.4

Figures 4.1 and 4.2 show the simulated turbine speed compared with the measured speed using only $wind_2$ or $wind_3$ respectively. Anemometer $wind_3$ of Fig. 4.2 clearly has a better high frequency response than does anemometer $wind_2$ of Fig. 4.1. However, anemometer $wind_3$ does not respond well to low wind speeds and returns a zero reading

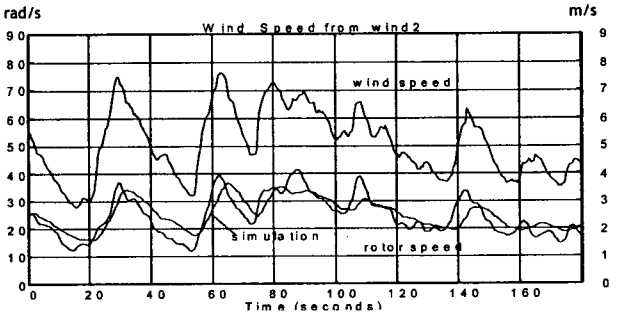

Figure 4.1 Comparison of the simulated turbine rotor speed with the measured speed using the measured wind speed data from $wind_2$. Correlation between simulation and measured turbine speed is 83% measured over 10 minutes.

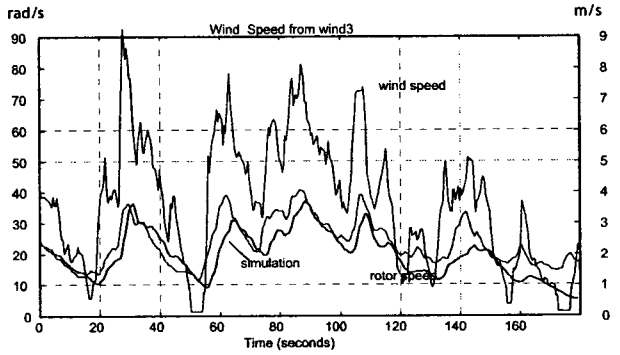

Figure 4.2 Comparison of the simulated turbine rotor speed with the measured speed using the measured wind speed data from $wind_3$. Correlation between simulation and measured turbine speed is 82% measured over 10 minutes.

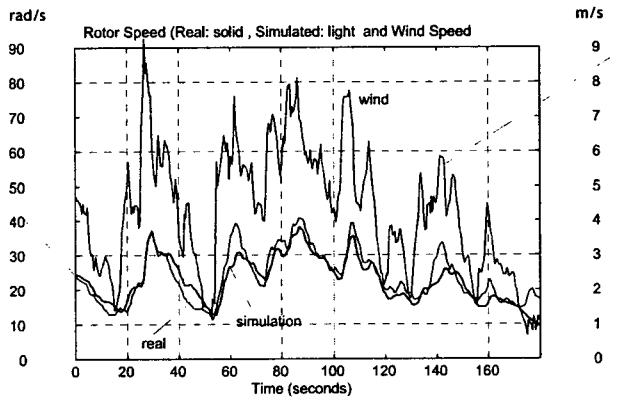

Figure 4.3 Comparison of the simulated turbine rotor speed with the measured speed using the measured wind speed data and adding in the frequencies above 0.08Hz from anemometer $wind_3$. Correlation between simulation and measured turbine speed is 91% measured over 10 minutes.

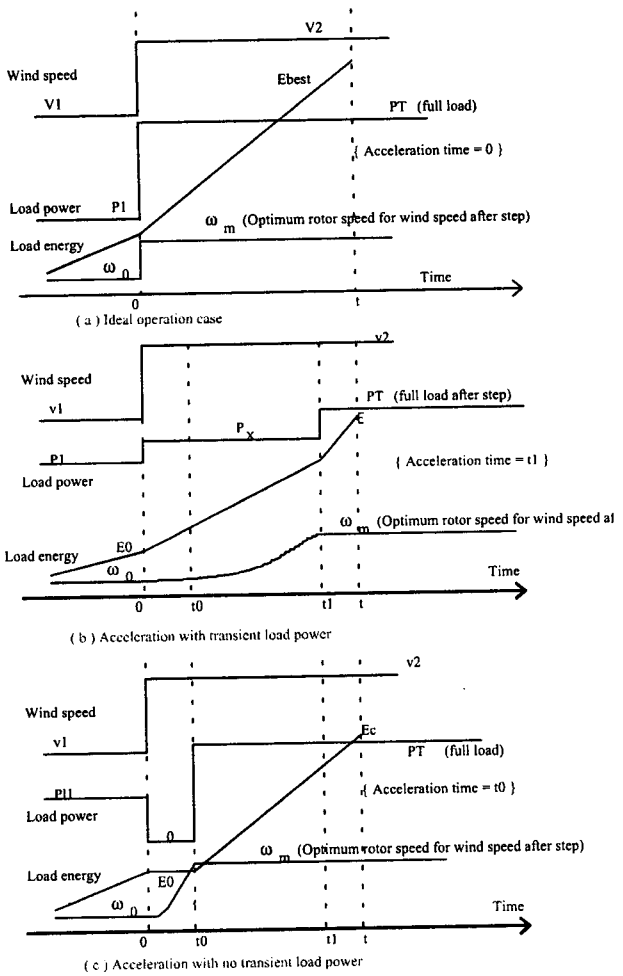

Figure 5.1 (a) ideal operation (maximum power coefficient maintained at all times), (b) operation with some transient load, and (c) operation with no transient load.

below about 4m/s (Fig. 4.2 at 55 seconds). But since the correlation coefficient is only about 83% for both cases, neither is acceptable.

Anemometer *wind*$_3$ does seem to have a result similar to a phase lag, which tends to reduce the simulated rotor speed below that of the measured result. This indicates that the turbine may have a higher frequency response than this anemometer. However, anemometers *wind*$_1$ (not shown) and *wind*$_2$ are clearly unable to respond to the higher wind frequencies, and often predict a too low rotor speed (and hence power output).

A heuristic iterative process was then used to combine the anemometer readings. It was found that geometrically averaging the wind speeds and adding in the frequencies above 0.08Hz from anemometer *wind*$_3$ was effective in producing a good match between simulation and experimental results. The result is shown in Fig. 4.3, with a correlation coefficient between the measured and simulated rotor speeds of 91%. This result validated the wind speed measurement algorithm [Harrap '93].

5.0 IMPROVED ENERGY EXTRACTION FROM STEP WIND SPEED CHANGES

Once the wind speed measurement algorithm was finalised, the investigation turned to consider how a turbine controller could be optimised to maximise the energy extracted under turbulent wind conditions.

As is clear the from the wind speed measurements of the Figs. 4.1 to 4.3, wind speeds can change very rapidly. If the wind turbine remains uncontrolled during such changes, it is known that the turbine will most likely operate suboptimally, because it does not maintain an optimum tip speed ratio. The problem then becomes how to determine an optimal control strategy to improve on this situation.

For simplicity, a step wind speed change was investigated as a limiting example. Then the turbine response was investigated with various levels of constant output power maintained during the speed transient event (ie. until the turbine accelerated to the optimum turbine tip speed ratio at the new wind speed).

Fig 5.1 shows the expected result that maximum turbine acceleration will be achieved with a step rise in wind speed when the turbine load is a minimum. Conversely, it would also be expected that maximum turbine deceleration will occur for a step reduction in wind speed when the turbine load is maximum.

Fig. 5.2 clearly shows that for step rise in wind speed, the

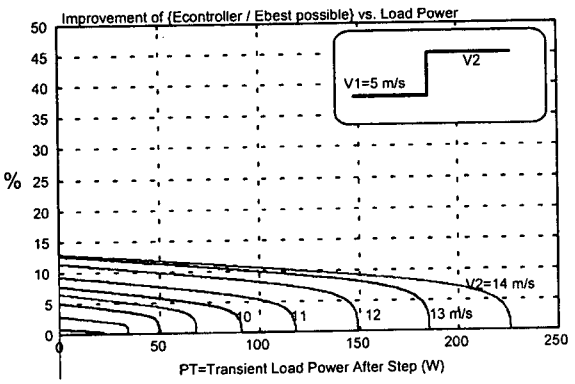

Figure 5.2 Simulation results of the improvement in the extracted energy under different transient loads during a step rise in wind speed.

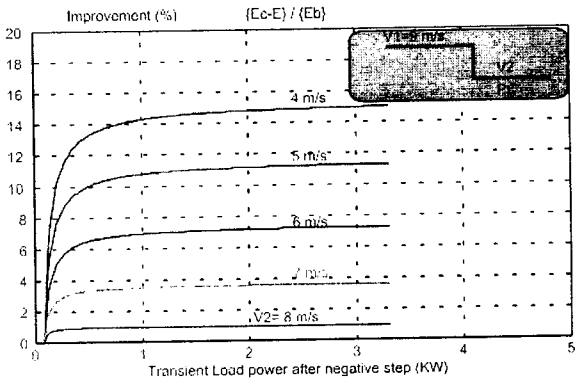

Figure 5.3 Simulation results of the improvement in the extracted energy under different transient loads during a step reduction in wind speed.

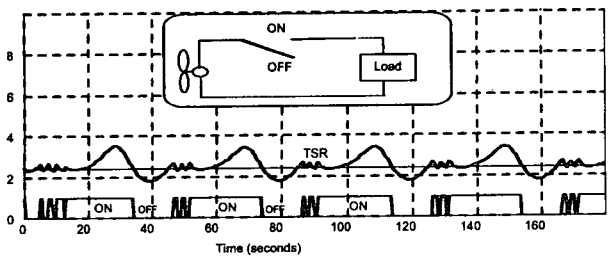

Figure 5.4 Sliding mode hysteresis controller operation. The switch is turned on/off when the tip speed ratio is greater/less than the threshold.

optimum strategy is to reduce the turbine load to zero during the time it takes for the turbine to return to the optimum tip speed ratio (and hence achieve its maximum power coefficient).

For a step reduction in wind speed, Fig. 5.3 shows that the converse is true, i.e. the greater the turbine load that can be applied, the better. This is because this load causes the turbine to decelerate as quickly return to the optimum tip speed ratio and therefore to its maximum power coefficient.

These results suggest a sliding mode controller operating to keep the turbine tip speed ratio within a band around its optimum value, would be an appropriate solution for this problem. A practical implementation of such a system is a conventional hysteresis controller, which switches the turbine load between zero and maximum as the tip speed ratio varies (Fig. 5.4) between 2.3 to 2.5, to keep it within 0.1 of the optimum tip speed ratio. Note that when the tip speed ratio is not within this band, the controller has saturated and control has been lost.

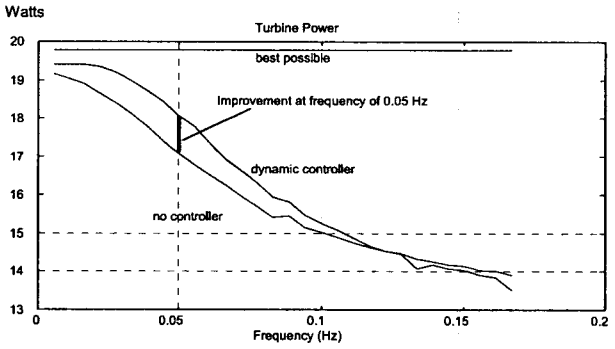

Figure 6.1 Simulated average turbine power versus different frequencies in the sinusoidal wind (5+3sinωt).

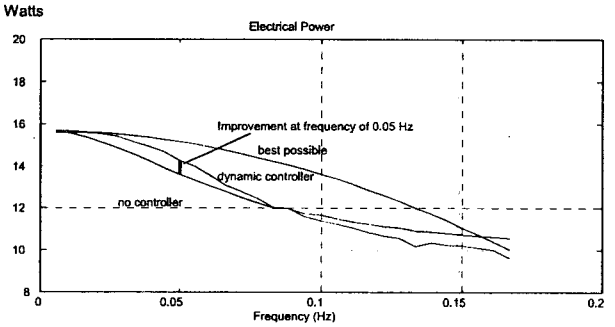

Figure 6.2 Simulated average electrical power for different frequencies of the sinusoidal wind speed (5+3sinωt).

6.0 OPERATION OF THE DYNAMIC WIND TURBINE CONTROLLER

Since any particular interval of wind speed can be represented as a Fourier series, the next step of the investigations was to evaluate the controller in simulation using sinusoidal wind speeds and plotting the average mechanical and electrical power obtained.

The results are shown in Fig. 6.1 for the mechanical power and Fig 6.2 for the electrical power. Fig. 6.1 shows that the turbine and the controller have a frequency response such that above about 0.12Hz, there ceases to be any advantage in using the dynamic controller. However, for the electrical output power (Fig 6.2), the cut-off frequency is lower at 0.08Hz (this somewhat unexpected result relates to the increased generator copper losses that occur as the generated output power increases, and is not explored further in this paper).

Hence if the combined wind speed measurement is further filtered by a low pass 0.12Hz filter (Fig. 6.3) before being passed to the controller, it will not attempt to respond to high frequency wind speed components.

Fig 6.4 shows the simulated gain in energy output that would be expected from the controller taking all these ideas into consideration. The result is a 4% energy gain over the 180 seconds of recorded wind speed data that was simulated.

7.0 FIELD EXPERIMENTAL RESULTS

Field trials were conducted for the system, where the control strategy was used for every alternate 10 minutes over a 24 hour period, and in the other 10 minute period, the turbine was directly connected to its load. The two wind

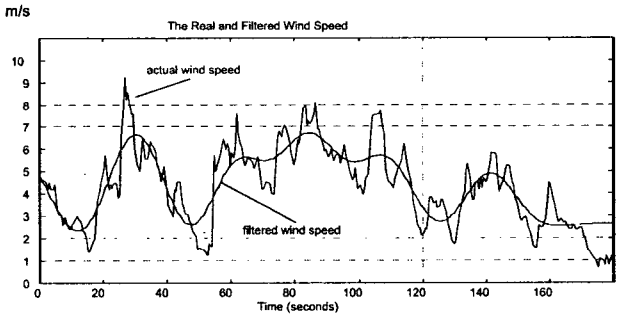

Figure 6.3 The prerecorded wind speed waveform and its filtered waveform.

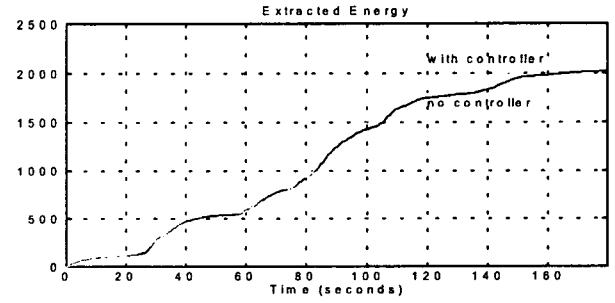

Figure 6.4 Energy generated by the turbine with and without the controller - simulation.

speeds of the alternative periods were found to have a correlation coefficient of 97%, which gave confidence that any energy differences measured were caused by controller action rather than wind speed variations.

The initial field trials measured an energy extraction improvement of only a disappointing 1.5%. This was then identified as being caused by a high cable resistance between the equivalent battery load and the turbine, that limited the load that could be applied to the turbine. When the load was replaced by a 6 Ω resistor, much better results were obtained, as a higher load could now be applied. This resulted in a dramatic improvement of nearly 50% in the turbine energy output, and an approximate 20% increase in the electrical energy output, as shown in Fig. 7.1. (Note that the electrical energy improvement was reduced compared to the turbine energy improvement because of the significant generator resistive losses).

8.0 CONCLUSION

Using a detailed model of a wind turbine system, which was capable of representing the turbine performance under dynamic wind conditions, a strategy for maximising the energy output from positive and negative wind speed step changes has been developed. For a step rise in wind speed, the strategy is to allow the turbine to accelerate with no load. For a step reduction in wind speed, the strategy is to apply maximum load to decelerate the turbine as quickly as possible. In each case the strategy extracts the maximum possible energy.

The control strategy has been implemented using a sliding mode based hysteresis controller, which switches the turbine between zero and maximum load as the turbine tip speed ratio varies around its optimum ratio. The operation of the controller has been verified in simulation using wind speed records and a precise model of the turbine and generator. Field trials were then implemented to investigate the operation of the controller in a practical situation.

The results obtained showed a disappointing result of only 1.5% gain when feeding into a battery equivalent load, but quite a significant increase of 50% in turbine energy and 20% in electrical energy when feeding into a resistive load. It was then identified that these differences were primarily because of a poor generator/load match for the battery equivalent load, which masked the gains that could be achieved by the new control strategy.

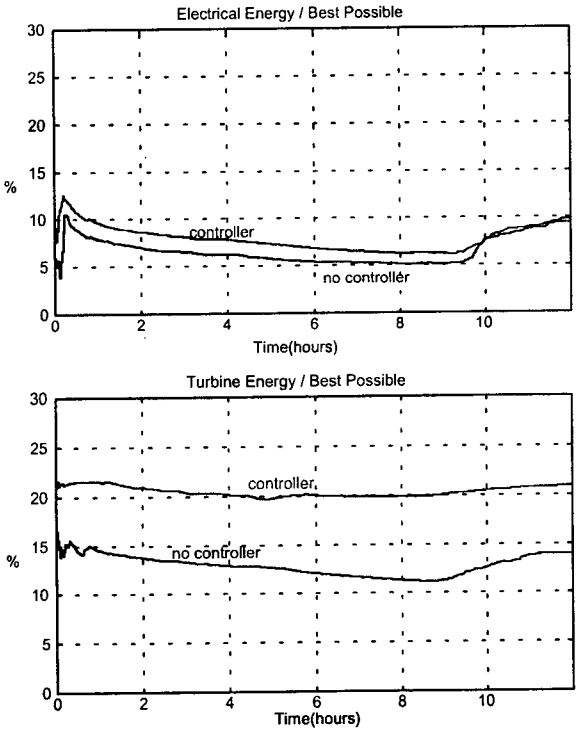

Figure 7.1 a) the measured improvement in the normalised electrical energy. b) the measured normalised improvement in the turbine energy.

9.0 REFERENCES

Borowy B.S. and Salameh Z.M. (1997), "Dynamic Response of a Stand Alone Wind Energy Conversion System with Battery Energy Storage to a Wind Gust", *IEEE Transactions on Energy Conversion, v12, n1, p73-78.*

Harrap M. (1993), "Ph.D. Thesis, Chapter 3, Field Tests with the Experimental Aero Generator - A Description", *School of Aerospace and Mechanical Engineering, University College, Australian Defence Force Academy.*

Leithead W.E. (1989), "Variable Speed Operation - Does it Have Any Advantages?", *Wind Engineering, v13, n6, p302-314.*

McIver A.D., Freere P., Holmes D.G. (1995), "Grid Connection of a Variable Speed Wind Turbine", *Wind Energy Workshop, Monash University*, 1995.

Press W.H., Teukolsky S.A., Vetterling W.T. and Flannery B.P. (1992), "Numerical Recipes in FORTRAN (the Art of Scientific Computing)", *Cambridge University Press.*

10.0 APPENDIX – TURBINE SYSTEM DETAILS

Cable Resistance between turbine and battery load = 2.6 Ω

Generator Backemf

ω= rotor speed V_1 = fundamental generator voltage

V_3 = 3rd harmonic generator voltage

$$V_1 = \sqrt{2} \times [0.6502\omega + 0.4156] \times \mathrm{Sin}(4.\omega.t)$$

$$V_3 = \sqrt{2} \times [0.0578\omega + 0.0531] \times \mathrm{Sin}(3 \times 4.\omega.t) \qquad (10\text{-}1)$$

Friction

P_{in} = friction power loss = $D\omega^2$

$$D = \text{friction coefficient} = 0.002 + 0.01 \times e^{-\omega/28} \qquad (10\text{-}2)$$

Inertia

J = inertia M = mass of generator rotor

m = mass of blade

x_1 = radius of generator x_2 = radius to end of blades

$$J = \frac{1}{2} \times M \times X_1^2 + 6 \times \frac{m}{3 \times (X_2 - X_1)} \times (X_2^3 - X_1^3) = 0.1717 \mathrm{Kgm}^2 \qquad (10\text{-}3)$$